



The silicone depletion in combination products induced by biologics

Fabian Moll^a, Karoline Bechtold-Peters^b, Wolfgang Friess^{a,*}

^a Pharmaceutical Technology and Biopharmaceutics, Department of Pharmacy, Ludwig-Maximilians-Universität München, 81377 Munich, Germany

^b Technical Research and Development, Novartis Pharma AG, 4002 Basel, Switzerland

ARTICLE INFO

Keywords:

Syringe functionality
Silicone oil
Protein formulations
Biopharmaceutics
Pre-filled syringes
Surface rheology
Silicone oil detachment

ABSTRACT

Silicone oil (SO) migration into the drug product of combination products for biopharmaceuticals during storage is a common challenge. As the inner barrel surface is depleted of SO the extrusion forces can increase compromising the container functionality. In this context we investigated the impact of different formulations on the increase in gliding forces in a spray-on siliconized pre-filled syringe upon storage at 2–8 °C, 25 °C and 40 °C for up to 6 months. We tested the formulation factors such as surfactant type, pH, and ionic strength in the presence of one monoclonal antibody (mAb) as well as compared three mAbs in one formulation. After 1 month at 40 °C, the extrusion forces were significantly increased due to SO detachment dependent on the fill medium. The storage at 40 °C enhanced the SO migration process but it could also be observed at lower storage temperatures. Regarding the formulation factors the tendency for SO migration was predominantly dependent on the presence and type of surfactant. Interestingly, when varying the mAb molecules, one of the proteins showed a rather stabilizing effect on the SO layer resulting into higher container stability. In contrast to the formulation factors, those different stability outcomes could not be explained by interfacial tension (IFT) measurements at the SO interface. Further characterization of the mAb molecules regarding interfacial rheology and conformational stability were not adequately able to explain the observed difference. Solely a hydrophobicity ranking of the molecules correlated to the stability outcome. Further investigations are needed to clarify the role of the protein in the SO detachment process and to understand the cause for the stabilization. However, the study clearly demonstrated that the protein itself plays a critical role in the SO detachment process and underlined the importance to include verum for container stability.

1. Introduction

Ready-to use primary packaging systems like pre-filled syringes are of particular importance for biopharmaceuticals as they enable the patient to administer the drug by himself, ease application for health care professionals and improve drug safety. A critical aspect in this context is the presence of silicone oil (SO) in the drug product [1–3]. SO is sprayed on the inner barrel of glass containers to reduce the friction force between the rubber plunger and the glass barrel thereby enabling an easy and consistent administration of the drug [4,5]. However, SO is known to migrate into solution where it forms microdroplets that add up to the overall particle count and potentially interact with the API [6,7]. SO is discussed to increase the immunogenicity of injectables [8,9] and there

have been numerous reports about SO microdroplets found in the vitreous after injections into the eye potentially causing adverse effects [10]. Hence, trends in the development of novel packaging materials are to fix the applied SO by baking-on, cross-linking, or to reduce the sprayed-on amount of SO [11–14]. Unfortunately, lower SO levels in the barrel potentially result in higher extrusion forces already after filling or during storage, thus it is important to better understand the process of SO detachment to define packaging materials that ensure functionality and safety of the combination product over the complete storage time.

The functionality of combination products over storage is impacted by the fill medium [15,16]. The increase in friction force caused by SO depletion from the container surface is triggered by surface active ingredients. The presence and a higher concentration of polysorbate 80

Abbreviations: 3D-LSM, 3D-Laser Scanning Microscope; CMC, Critical Micelle Concentration; E', Storage Modulus; E'', Loss Modulus; Fmax, Maximum Extrusion Force; FTIR, Fourier Transform Infrared Spectroscopy; HIC, Hydrophobic Interaction Chromatography; HPW, Highly Purified Water; IFT, Interfacial Tension; mAb, Monoclonal Antibody; PAT, Profile Analysis Tensiometer; PS, Polysorbate; Px, Poloxamer; SO, Silicone Oil; WI, White Light Interferometry; WLI, Combined White Light and Laser Interferometry.

* Corresponding author at: Department of Pharmacy, Pharmaceutical Technology & Biopharmaceutics, Butenandtstrasse 5, 81377 Munich, Germany.

E-mail address: wolfgang.friess@lrz.uni-muenchen.de (W. Friess).

<https://doi.org/10.1016/j.ejpb.2024.114418>

Received 8 May 2024; Received in revised form 2 July 2024; Accepted 15 July 2024

Available online 28 July 2024

0939-6411/© 2024 The Author(s). Published by Elsevier B.V. This is an open access article under the CC BY-NC license (<http://creativecommons.org/licenses/by-nc/4.0/>).

(PS 80) negatively impact the container stability and induce higher particle formation [17]. Furthermore, formulations containing poloxamer 188 (Px188) exhibit a lower tendency to detach SO compared to PS 80 [16,18]. This effect is linked to the interfacial properties of the fill medium. With increasing PS 80 concentrations the interfacial tension (IFT) between the formulation and SO decrease. In addition, PS80 decreases the IFT more effectively than Px188 [16,19–21]. Besides the surfactant, Fang et al. reported that the buffer system, pH and tonicity agents impact syringe functionality upon storage [18]. However, this was demonstrated predominantly for placebo and without monitoring the state of the SO layer or IFT. Therapeutic proteins constitute surface active molecules which adsorb to interfaces, decrease the IFT as well as form viscoelastic films and are known to interact with the SO layer [6,22–28]. Correspondingly, a monoclonal antibody (mAb) verum shows higher SO particle concentrations in the drug product as compared to a placebo and a mAb concentration dependent increase in gliding forces has been reported [6,16,29]. Although protein adsorption can be inhibited in formulations by surfactants, co-adsorption of mAbs at the interface occurs [19,26,30–32]. The interfacial storage modulus of the mAb film formed the SO interface correlates with the mAb adsorption and aggregation propensity at the SO interface [25,33]. But further thorough investigation of the formulation variables including the protein properties are still necessary.

The purpose of this study was to further identify formulation related factors which lead to a reduced stability in siliconized syringes due to SO migration. Compared to previous reports, we systematically tested different formulation variables a mAb and compared 3 different mAbs in the same formulation. We hypothesized that the IFT between formulation and SO to correlate with the increase in extrusion forces upon storage, also in the presence of the proteins. Formulation factors included protein concentration, pH, surfactant type (polysorbate 20 (PS20) and Px188) and concentration as well as ionic strength. A change of the pH and ionic strength are known to influence adsorption behaviour of proteins to accessible surfaces and thus the container stability in terms of functionality could be influenced indirectly [34–37]. We monitored the extrusion forces upon storage at 2–8 °C, 25 °C and 40 °C for up to 6 months. The residual SO amount and the SO layer thickness in the barrels were determined by Fourier-transform infrared spectroscopy (FTIR) and interferometry measurements. 3D-laser scanning microscopy (3D-LSM) was utilized to take images of the silicone layer from outside the barrel at all the study timepoints. The IFT between the formulations and SO were obtained with a profile analysis tensiometer (PAT). We further characterized the formulations and mAbs in terms of interfacial rheology properties. As an impact of the mAb on the SO detachment became obvious, the proteins were further characterized in terms of hydrophobicity and conformational stability with the aim to find protein characteristics which explain and potentially predict the protein induced SO detachment. Both parameters are considered important in the adsorption process of mAbs to surfaces [35,38–40].

2. Materials and methods

2.1. Materials and methods

2.1.1. Chemicals

Following chemicals were used: L-histidine, L-histidine monohydrochloride monohydrate, polysorbate 20 (PS20), NaCl (Merck KGaA, Darmstadt, Germany), trehalose (Ferro Pfanstiehl, Waukegan, IL, USA), sucrose (Sigma-Aldrich Chemie GmbH, Steinheim, Germany) and Poloxamer 188 (BASF, Ludwigshafen, Germany).

2.1.2. Sample preparation

Four different IgG1 monoclonal antibodies were kindly provided by Novartis AG (Basel, Switzerland). mAb 2, 3 and 4 were obtained in histidine-buffers without further excipients. mAb 1 was obtained already finally formulated at 120 mg/mL in histidine buffer (His)

containing trehalose and 0.02 % (w/v) PS20. Vivaflow® 50 cross flow cassettes with a 50 kDa MWCO PES membrane (Sartorius AG, Goettingen, Germany) were used to concentrate the other protein solutions or exchange the buffer system. Buffer solutions were prepared with highly purified water and pH was checked with a Mettler Toledo MP220 pH meter (Mettler Toledo, Greifensee, Switzerland). After final formulation, concentration was checked using UV-Vis spectrophotometer Nano-Drop™ (Thermo Scientific, Wilmington, Delaware, USA). To investigate the impact of formulation variables, mAb 4 was formulated varying protein concentration, pH, ionic strength, and surfactant type and concentration (Table 1). mAb 2 and 3 were formulated according to the formulation of mAb 1 including 0.02 % (w/v) PS 20. For all protein formulation, an accordingly formulated placebo was prepared. The protein solutions were filled into 1 mL long BD Neopak™ syringes with 27G ½" staked-in needles (BD Medical – Pharmaceutical Systems, Le Pont-de-Claix, France) and containers were closed with NovaPure® Syringe Plungers (West Pharmaceutical Services, Inc., Exton, PA, USA) under laminar air flow. The plungers were all set to the same height using an insertion jig. Prior filling all solutions were sterile filtrated using vacuum filtration units with a 0.2 µm PES filter membrane (VWR International GmbH, Darmstadt, Germany).

2.2. Stability study

Syringes filled with mAb 1–3 were stored without agitation at 40 °C and 2–8 °C for up to 6 months as well as at 25 °C for up to 3 months, mAb 4 formulations were stored for up to 3 months at 40 °C. At designated timepoints functionality, particle formation, silicone distribution and content per barrel as well as silicone layer morphology were investigated.

2.2.1. Functionality

Functionality was investigated using a Texture Analyzer TA.XT Plus (Stable Micro Systems Ltd., Surrey, UK). The containers were expelled with a velocity of 190.2 mm/min until a trigger force of 30 N. The maximum force required for the distance 0–35 mm was set as the maximum extrusion force (Fmax). Extrusion was automatically stopped, when the upper limit of 30 N was reached and such container systems were declared as “failed“ (n ≥ 5).

Table 1

Overview of verum and placebo formulations of mAb 4 tested (30 mM His, 270 mM sucrose). *Only tested as placebo.

Abbreviation	Protein Concentration	pH value	Ionic Strength	Surfactant
Standard	75 mg/ml	6.0	-	0.06% (w/V) PS20
Low mAb	5 mg/ml	6.0	-	0.06% (w/V) PS20
Middle mAb	40 mg/ml	6.0	-	0.06% (w/V) PS20
High mAb	120 mg/ml	6.0	-	0.06% (w/V) PS20
Low pH	75 mg/ml	5.0	-	0.06% (w/V) PS20
High Ion	75 mg/ml	6.0	140 mM NaCl	0.06% (w/V) PS20
High Surfactant	75 mg/ml	6.0	-	0.12% (w/V) PS20
w/o Surfactant	75 mg/ml	6.0	-	-
Px188	75 mg/ml	6.0	-	0.06% (w/V) Px188
High Px188	75 mg/ml	6.0	-	0.40% (w/V) Px188

2.2.2. Subvisible particle analysis (SvP-analysis)

Particles in the product were monitored using a FlowCam 8100 (Fluid Imaging Technologies, Inc., Scarborough, ME, USA) equipped with a 10× magnification lens. Samples were collected during the functionality measurements in pre-rinsed Eppendorf® tubes and particle > 1 µm concentration was evaluated using 150 µl at a flowrate of 100 µl/min (n ≥ 4).

2.2.3. Silicone oil distribution by combined white light and laser interferometry (WLI) and white light interferometry (WI)

A RapID Layer Explorer UT (rap.ID Particle Systems GmbH, Berlin, Germany) was used to evaluate the silicone oil distribution in the barrel. Prior to measurements, the syringes were emptied after carefully removing the plunger with tweezers. The barrels were subsequently rinsed with 1 mL highly purified water (HPW) at least 3 times and firmly dried. After baseline recording of a non-siliconized syringe 8 lines of 40 mm per barrel with a resolution of 0.4 mm/step were recorded to determine the silicone layer thickness along the barrel. In the study evaluating the mAb effect combined white light and laser interferometry (WLI) was used (UT Mode/LOD = 20 nm), whereas in the formulation effect study syringes were evaluated using white light interferometry (WI) (BI Mode/LOD = 80 nm). Calculating the silicone layer thickness silicone depletion was evaluated based on the datapoints 35 – 100. Datapoints below limit of detection were counted as 20 nm respectively 80 nm depending on the method used. Samples declared as T0 display syringes not filled (n = 3).

2.2.4. Silicone layer morphology

The silicone layer of syringes emptied and cleaned as described above was assessed with a Keyence VK-X250 3D-Laser Scanning Microscope (Keyence International NV/SA, Mechelen, Belgium). After focusing on the silicone layer from outside images were taken alongside the barrel with a CF Plan 10×/0.30 Nikon OFN WD 16.5 objective. Seven images in the middle of the barrel were stitched together with the VK Image Stitching software (version 2.1.1.0).

2.2.5. Silicone oil quantification by fourier transform infrared spectroscopy (FTIR)

The silicone oil amount per barrel was quantified via Fourier Transform Infrared Spectroscopy (FTIR) with a Bruker FTIR Tensor 27 (Bruker Corp., Billerica, MA, USA) after emptying and cleaning the syringes as described above and following a method developed by Funke et al. [41]. Briefly, the silicone oil was extracted twice per barrel with 700 µl n-heptane. Therefore, plungers were inserted with the same jig used for the stability study and the syringes were rotated overhead for 20 min at 18 rpm. The solvent extracts were pooled in 2R vials and heptane was removed with a Flowtherm Evaporator (Barkey GmbH & Co.KG, Leopoldshöhe, Germany) at 100 °C and nitrogen flow of 100 mL/min. The dried extract was redissolved with 500 µl n-heptane and filled into a 250 µm path length transmission liquid cell. To obtain transmittance spectrum 100 scans with a resolution of 4 cm⁻¹ were recorded between the wavelengths 3000 to 900 cm⁻¹. After calibration (R² = 0.9999), silicone oil was quantified based on the area under the curve of the symmetrical Si-CH₃ deformation between 1280 and 1240 cm⁻¹ obtained by the Bruker OPUS software (Version 7.5.18). Samples declared as T0 display syringes not filled (n = 3).

2.3. Interfacial behaviour at silicone oil interface

The interfacial tension (IFT) at the silicone interface of the various fill mediums was determined with a PAT1M profile analysis tensiometer (SINTERFACE Technologies e.K., Berlin, Germany). A droplet was formed with a single capillary (2.1 mm) immersed in silicone oil (Dow Corning® 360 Medical Fluid 100 cSt, Dow Corning GmbH, Wiesbaden, Germany). Dynamic interfacial tension was recorded based on the captures of a video camera for at least 5000 s. For the samples mAb 1 – 3 the

droplet volume was oscillated after 5000 s (Amplitude 10 %) at 0.01 Hz, 0.02 Hz, 0.05 Hz, 0.1 Hz and 0.2 Hz. Fourier Transformation enabled the calculation of viscoelastic properties of the adsorbed surfactant and protein layers (storage modulus E' and imaginary modulus E''). Protein concentration was adjusted to 5 mg/mL for all PAT measurements (n = 3).

2.4. Conformational stability

The mAb unfolding was studied by nano differential scanning calorimetry (nanoDSF) at 1 mg/mL using a Prometheus® NT.48 (nanoTemper Technologies, Munich, Germany) at 1 °C/min from 20 °C to 100 °C. Fluorescence intensity at 350 nm was plotted against temperature and the apparent melting temperature of the protein was obtained from the maximum of the first derivative using the PR.ThermControl V2.1 software (nanoTemper Technologies, Munich, Germany) (n = 3).

Additionally, isothermal chemical denaturation (ICD) was used to characterize the protein physical stability following a method developed by Svilenov et al. [42]. Protein stock solutions (10 mg/mL in His-Buffer) were pipetted into a non-binding surface 384 well plate (Corning, USA) and mixed with the buffer and a denaturant stock solution (6 M guanidine hydrochloride) resulting in different denaturant concentration and a constant protein concentration of 1 mg/mL. Pipetting and mixing were performed with a 12.5 µL and 125 µL Viaflo pipette and the Viaflo Assist (Integra Biosciences, Konstanz, Germany). After sealing the microplate, the samples were incubated at room temperature for 27 h and intrinsic fluorescence was determined at 350 nm with a Fluostar Omega microplate reader (BMG Labtech, Ortenberg, Germany). The data was plotted against denaturant concentration with the CDpal software (Version 2.15) [43] and the autofit function was used to evaluate the approximate C_m values of the curves (n = 3).

2.5. Hydrophobicity

Hydrophobic interaction chromatography (HIC) was used to evaluate protein hydrophobicity. Protein samples were analyzed on an Agilent 1200 device (Agilent Technologies GmbH, Böblingen, Germany). MAb samples were diluted with ammonium sulphate buffer to a final concentration of 0.33 mg/mL prior analysis. A total mAb amount of 20 µg was injected onto a 35 × 4.6 mm TSKgel Butyl-NR column from Tosoh Bioscience GmbH (Darmstadt, Germany) and eluted at a flow rate of 1 mL/min at 25 °C. After the equilibration of the column for 2 min with buffer A (20 mM His/HCl, pH 5.4 containing 1.5 M (NH₄)₂SO₄, concentration of buffer B (20 mM His/HCl, pH 5.4) was increased linearly from 0 – 100 % in the following 66 min (t_{gradient}). MABs were detected with a G1314B UV detector at 280 nm. The results are presented as the quotient of retention time and t_{gradient}.

3. Results

3.1. Stability study – variation of formulation

After filling spray-on siliconized syringes with mAb 4 formulations differing in protein concentration, pH, surfactant type, concentration as well as ionic strength (Table 1), containers were stored at 40 °C for 3 months. Next to the progress in gliding forces, SvP count of expelled samples was evaluated. SO migration was monitored by quantifying residual SO amount per barrel after extraction and SO layer thickness measurements. Both results were supported by 3D-LSM of the inner SO surface.

3.1.1. Functionality

The F_{max} of the protein and placebo samples increased over storage dependent study. This included the functionality failure of a broad number of syringes at the end of the stability study after 3 months at 40 °C (Fig. 1). The increase in extrusion force was dependent on the

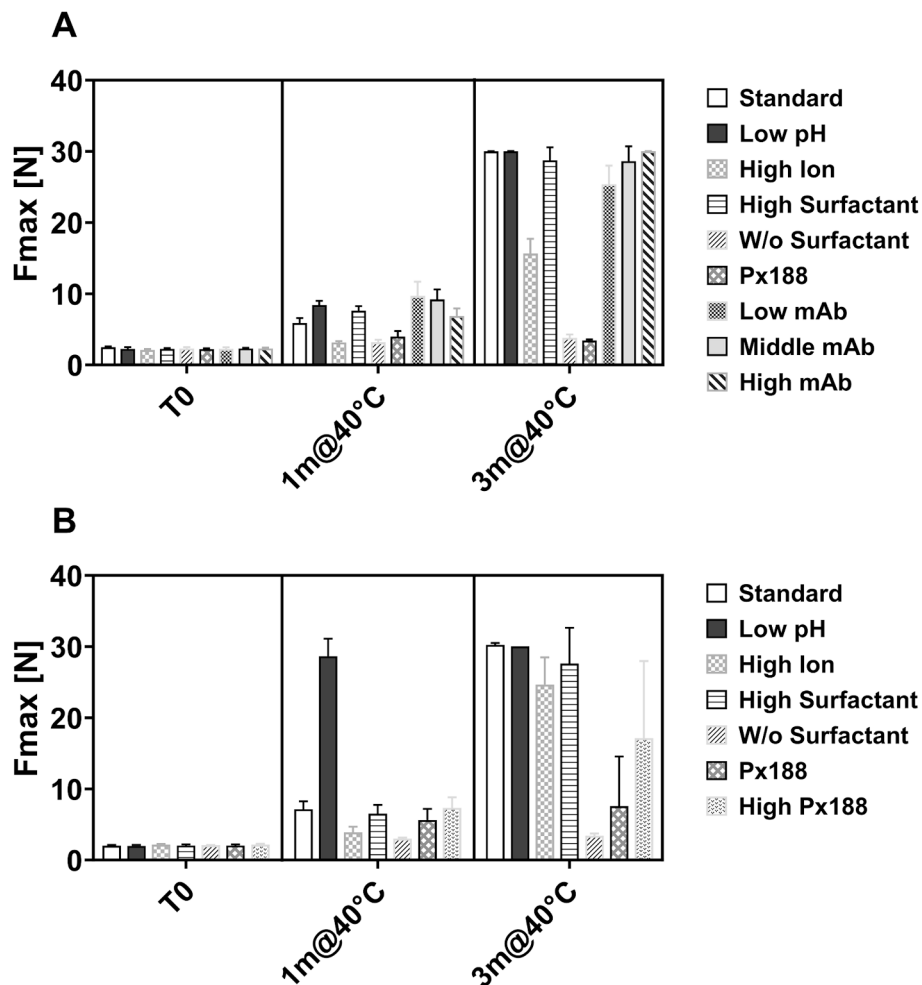


Fig. 1. Maximum extrusion forces (F_{max}) of syringes after storage at 40 °C of different mAb 4 [A] and placebo [B] formulations.

formulation filled in. At T0 all samples showed similar F_{max} values between 2.1 N and 2.5 N, which increased to 6 N and 10 N for most of the samples after 1 month at 40 °C. The samples without surfactant and with Px188 showed a smaller increase towards values of 3.2 ± 0.2 N and 4.0 ± 0.8 N respectively. Interestingly, also the syringes containing a formulation with higher ionic strength were still easier to expel with F_{max} values of 3.1 ± 0.2 N. After 3 months, the extrusion force was massively increased to 25 N to 30 N for the syringes except for the ones containing either no surfactant or Px188, which staged at approximately 3 N, and the high ionic strength formulation with 15.6 ± 2.1 N.

These results agree with the F_{max} results of the corresponding placebos. In some cases, the placebo solution showed higher extrusion force values after storage. For instance, the lower pH placebo formulation showed an increase from 2.0 ± 0.1 N to 28.6 ± 2.5 N already after 1 month at 40 °C and for the Px188 placebo sample a higher F_{max} of 7.6 ± 7.0 N was detected after 3 months. An additional formulation with a higher Px188 concentration (0.4 % (w/v)) resulted in F_{max} of 17.1 ± 10.8 N, which was higher than with 0.06 % (w/v) Px188, but still lower compared to the PS20 containing samples.

3.1.2. SvP-analysis

The particle count of the expelled samples was assessed with flow imaging and served as indicator for silicone oil migration into the product (Fig. 2). Formulations without PS20 or containing Px188 did not show an increase in particle concentration upon storage at all. At maximum $66,000 \pm 19,000$ particles $> 1 \mu\text{m/mL}$ were detected in verum and $36,000 \pm 25,000$ particles $> 1 \mu\text{m/mL}$ in placebo. All PS20

containing samples showed enhanced particle concentrations after expelling. In general, placebo solutions for this group showed lower particle counts compared to protein containing solutions as they did not exceed values $> 3.5 \times 10^5$ particles $> 1 \mu\text{m/mL}$. In comparison, 5 out of the 7 protein samples showed values of $> 1 \times 10^6$ particles $> 1 \mu\text{m/mL}$. Particularly high particle concentrations were detected for the protein formulation with a higher PS20 concentration (High Surfactant/ 0.12 % (w/v)), which reached values up to 4.8×10^6 particles $> 1 \mu\text{m/mL}$ after 3 months storage. Lower particle concentrations were found for the solution containing higher mAb concentration (120 mg/mL) and the lower pH 5.

3.1.3. Silicone layer characterization

Silicone layer detachment upon storage could be demonstrated by silicone oil quantification with FTIR as well as by interferometry measurements at the silicone layer to determine its thickness. The solutions without PS20 or containing Px188 also at higher concentration showed a reduction of the silicone oil from approximately 200 μg SO per barrel to 120 – 160 μg after storage for 1 or 3 months (Fig. 3). For PS20 containing formulations the amount decreased to 50 – 80 μg after 1 month and approximately 30 μg after 3 months. Overall, the effect was similar for the verum and the placebo.

The results were reflected by silicone layer thickness measurements (Fig. 4). Silicone oil was hardly detectable in the samples except for the surfactant free and the Px188 containing formulations with most of the datapoints $< \text{LOD}$ already after 1 month at 40 °C. As all datapoints $< \text{LOD}$ were calculated as 80 nm, the boxes of samples with obvious

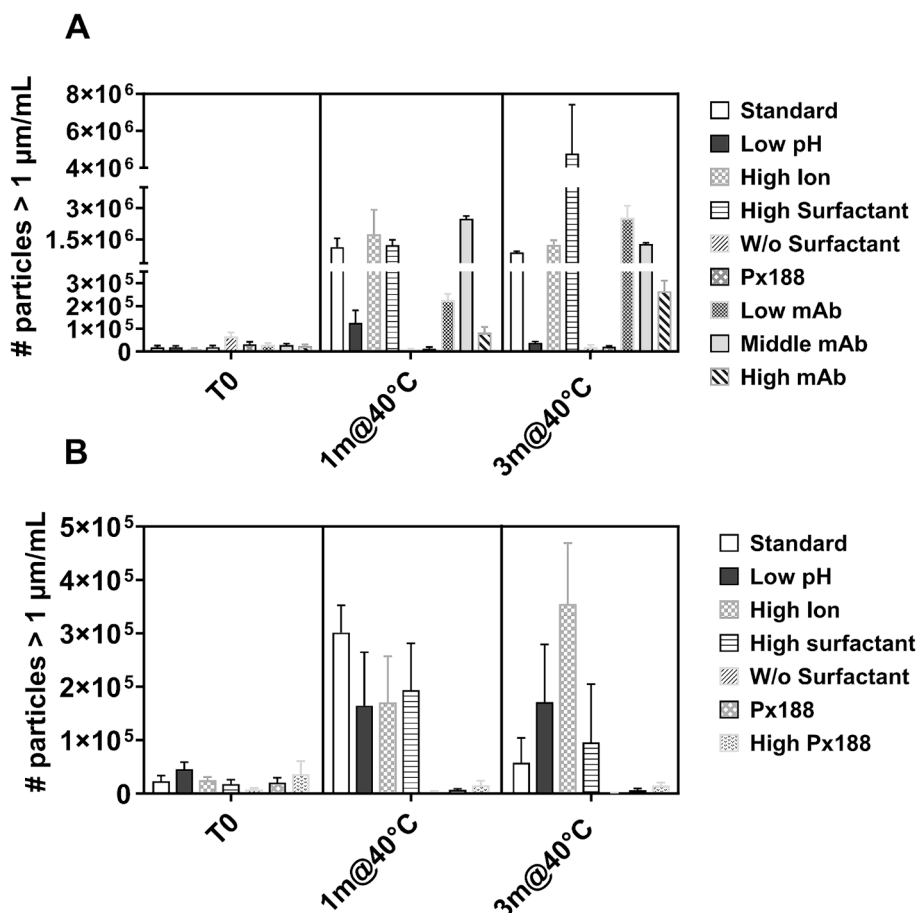


Fig. 2. Number of particles $> 1 \mu\text{m/mL}$ after storage at 40°C for different mAb 4 [A] and placebo [B] formulations.

depletion appear as a flat line. The Px188 concentration did not impact the change in silicone layer thickness. After 3 months the silicone layer height was further decreased for both the protein and placebo. In general, the presence of protein enhanced the decline of the layer thickness. Furthermore, silicone layer thickness for the Px188 containing as well as the standard formulation stored for 3 months was examined in UT mode (Supplementary Data – Figure S1); the majority of the datapoints detected for the standard formulation was $< \text{LOD}$ as well indicating no silicone at all at the inner barrel surface. The Px188 showed more silicone oil left and less depletion occurred with placebo.

3D-LSM confirmed the findings. At start, the SO formed blurred structures (Fig. 5), which were still partially present after 1 month (Supplementary Data – Figure S2) and vanished for PS20 containing samples after 3 months storage. Reminders of SO were still visible for the surfactant free and Px188 containing formulations.

3.2. Stability study – variation of the mAb molecule

After filling spray-on siliconized syringes with one formulation (Formulation mAb 1) but 3 different mAbs (mAb 1–3), containers were stored for up to 6 months at 40°C , 25°C and $2-8^\circ\text{C}$. Container stability as well as SO migration upon storage was monitored as abovementioned.

3.2.1. Functionality

Extrusion forces at T0 were low for all syringes with F_{max} between 2.3 N and 4.7 N. F_{max} of the mAb 1–3 solution and placebo filled syringes increased with storage (Fig. 6). Overall, the syringes filled with mAb 1 showed the most pronounced increase of F_{max} followed by placebo and mAb 2. F_{max} of syringes filled with mAb 3 increased least

and was still acceptable even after 6 months storage at 40°C .

After one month storage at 40°C , already 2 out of 6 placebo solution samples failed respectively they showed a $F_{\text{max}} > 30 \text{ N}$ (average F_{max} of $26.8 \pm 5.2 \text{ N}$ / Fig. 6). After 3 months at 40°C , 4 out of 6 syringes filled with mAb 1 failed reaching an F_{max} average of $29.8 \pm 0.3 \text{ N}$; placebo solutions completely failed at that timepoint. An increase became also evident for mAb 2 ($F_{\text{max}} 15.3 \pm 1.9 \text{ N}$) and mAb 3 ($F_{\text{max}} 11.1 \pm 0.9 \text{ N}$). The results after 6 months at 40°C were similar to the 3-month timepoint except for a further increase of F_{max} for the mAb 2 formulation to $22.4 \pm 1.6 \text{ N}$. For mAb 1 and placebo all syringes exceeded 30 N after 6 months at 40°C . Also, at lower storage temperatures F_{max} increased but no syringe failed after 6 months. In line with the 40°C storage results, mAb 1 and 2 showed markedly higher F_{max} values than mAb 3 also after storage at $2-8$ and 25°C . Interestingly, the placebo showed the least increase of all samples at the lower temperatures in contrast to storage at 40°C .

3.2.2. SvP-analysis

The concentration of particles $> 1 \mu\text{m}$ increased after storage at all temperatures (Fig. 7). After filling mAb 2, mAb 3, and placebo samples showed 18.000 to 25.000 particles $> 1 \mu\text{m/mL}$ and mAb 1 70.000 ± 29.000 particles $> 1 \mu\text{m/mL}$ on average. After 1 month at 40°C , mAb 1 and placebo samples contained around 200.000 particles $> 1 \mu\text{m/mL}$ and mAb 2 samples 380.000 ± 95.000 particles $> 1 \mu\text{m/mL}$, whereas mAb 3 samples stayed much lower with 40.500 ± 10.000 particles $> 1 \mu\text{m/mL}$. The particle concentrations did increase further at the 3- and 6-month timepoint for the mAb 2 and 3 samples. As the extrusion was not conducted completely for the mAb 1 and placebo at those timepoints, the results cannot be further compared (marked as x and y in Fig. 7). The failing of the syringes obviously decreased the particle count in the

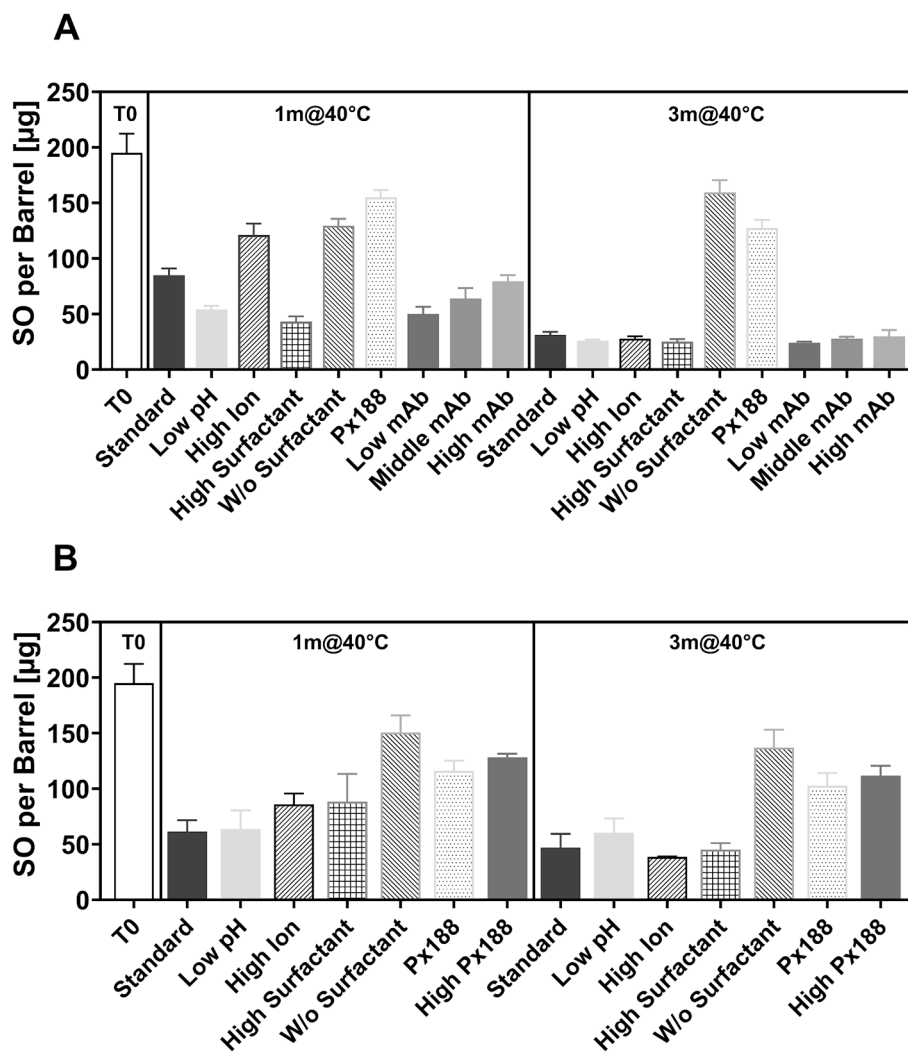


Fig. 3. SO amount per barrel by FTIR after storage at 40 °C of different mAb 4 [A] and placebo [B] formulations.

collected samples. After 3 months storage at 25 °C mAb 1, 2 and placebo showed increased particles levels and mAb 3 no change. At 2–8 °C after 6 months, the particle count was marginally increased in all samples at a similar level.

3.2.3. Silicone layer characterization

As shown for the variation of the formulation the increase in extrusion forces for syringes filled with different mAbs was linked to a steady decrease of the SO layer height on the inner barrel surface. Syringes filled with mAb 1, mAb 2 and placebo showed a rather similar decline of the SO amount over storage (Fig. 8) reaching values around 30 µg per barrel after 6 months at 40 °C. In contrast, the lowest values obtained for mAb 3 samples were around 90 µg per barrel. Results for the samples stored for 3 months at 25 °C were comparable to the 1-month timepoint at 40 °C. After 6 months at 2–8 °C the SO level for all samples was only half of the T0 value without obvious differences between the samples.

Corresponding results were obtained with interferometry. For mAb 1, mAb 2 and placebo solutions SO was hardly detectable after storage at 40 °C and 25 °C (Fig. 9). Starting at a median of approximately 160 nm for unfilled syringed the thickness dropped to 20 nm representing the LOD of the method. In contrast, the medians of syringes filled with mAb 3 ranged roughly between 58 and 73 nm throughout the stability study. Silicone oil detachment was less pronounced at 2–8 °C; still the decrease was less distinct for mAb 3. Furthermore, the inner barrel of syringes filled with mAb 1, mAb 2 or placebo showed the appearance of

the surface of a silicone oil free glass syringe in 3D-LSM already after 1 month storage at 40 °C (Fig. 10/ Supplementary Data – Figure S3). In contrast, the images of syringes filled with mAb 3 indicated presence of a SO layer although the inner surface appeared less smooth and congruent. After 3 months at 25 °C, SO still was visible for mAb 3 and placebo solution; after 6 months at 2–8 °C SO was still clearly visible for all samples.

3.3. Interfacial behaviour silicone oil interface

Interfacial tension and rheological measurements between the formulations and SO were performed looking for explanations of the difference in the outcome of the stability study with respect to both the formulation and the mAb effect.

3.3.1. Variation of the formulation

All PS20 containing samples showed the same progression of the IFT at the SO interface over time with a fast decline in the first 100 s to values of around 9 mN/m, which continued to decrease to 7 mN/m after 5000 s (Fig. 11). The corresponding placebo solution showed the same progression with slightly but consistently higher values. In contrast, Px188 containing samples induced IFT to decrease instantly to higher values of 20 mN/m without further change after the first 100 s and lower IFT values for the placebo solution. The formulations without surfactant showed a rather slow decline to values of 22.9 ± 0.7 mN/m after 5000 s,

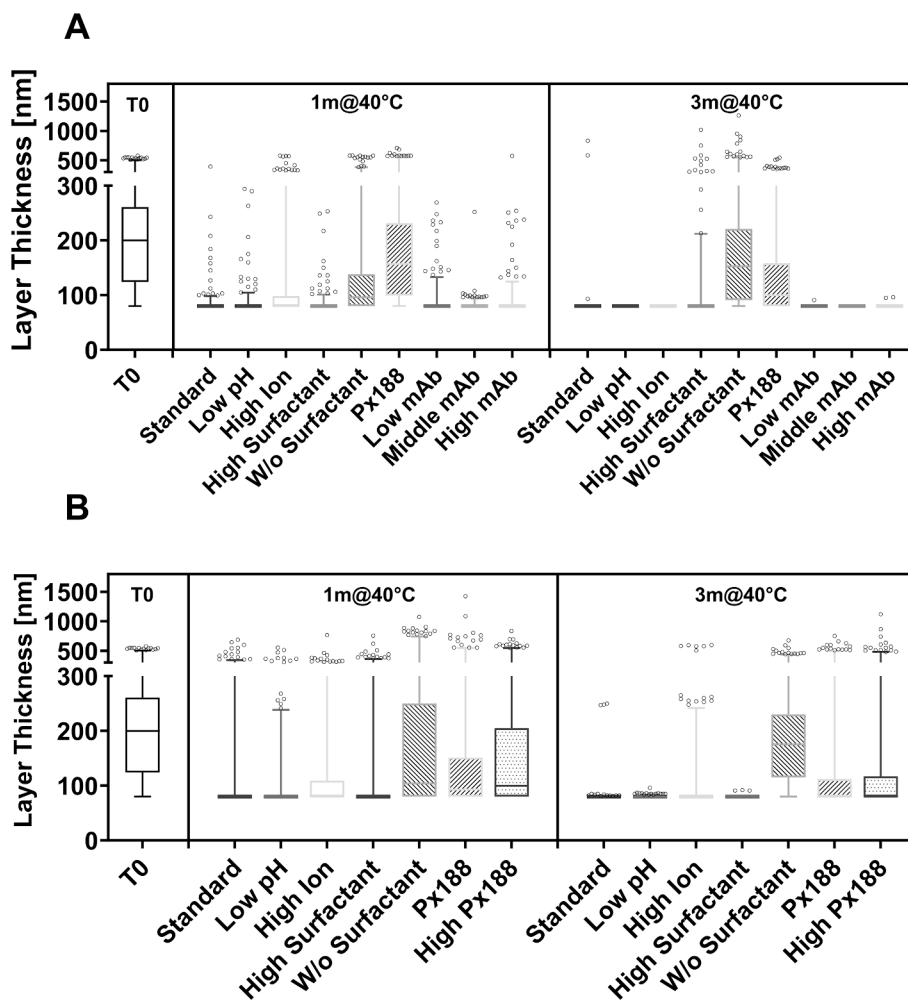


Fig. 4. SO layer thickness by WI after storage at 40 °C of different mAb 4 [A] and placebo [B] formulations displayed as box plots (Box. 25th – 75th percentile; Whiskers. 1th – 99th percentile/LOD. 80 nm).

whereas the IFT was stable for the surfactant free placebo at a value of 34 mN/m.

3.3.2. Variation of the mAb molecule

As seen for the formulation study, the presence of the surfactant predominantly determined the progression of the IFT at the SO interface over time thus resulting in a decline to 8 mN/m after 5000 s for all samples including the placebo compared to 37 mN/m of the surfactant free buffer (Fig. 12). Furthermore, no significant difference was observable in between the surfactant free mAb solutions (mAb 1 – 3) as they all decreased the IFT to approximately 26 mN/m after 5000 s. Dilational rheology measurements indicated the same viscoelastic properties of the films formed at the silicone interface for the actual formulations (Fig. 13, A) as there was no distinct difference in the storage (E') and loss modulus (E'') at different frequencies observable. Without the surfactant the elasticity of the different mAb films was similarly increased (Fig. 13, B).

3.4. Further mAb properties

The three different mAbs were further characterized and ranked in terms of solution viscosity, hydrophobicity, and conformational stability. The viscosity of the mAb 1 formulation was significantly higher with 14.2 ± 0.0 mPa*s compared to 5.8 ± 0.2 mPa*s and 5.0 ± 0.0 mPa*s for mAb 2 and 3. In addition, mAb 1 showed the highest hydrophobicity with a retention time quotient in HIC of 0.57 followed by mAb 2 and

mAb 3 with 0.49 and 0.44 respectively.

The ranking in terms of conformational stability obtained by isothermal chemical denaturation matched the results by thermal unfolding of the proteins with nDSF (Supplementary Data – Figure S4). mAb 1 was least stable with the earliest unfolding with a T_m of 71.6 ± 0.0 °C and a C_m of 2.1 ± 0.1 M, followed by mAb 3 with a T_m of 76.8 ± 0.1 °C and C_m of 2.3 ± 0.0 M, and mAb 2 showing a T_m of 79.0 ± 0.0 °C and C_m of 2.7 ± 0.1 M.

4. Discussion

The aim of the present study was to identify mAb formulation factors, which contribute to reduced storage stability by enhancing SO detachment from the container surface. To this end, we investigated the impact of different fill media upon long-term storage of spray-on siliconized pre-filled syringes.

At first, we varied the mAb formulations in terms of excipient type and concentration. Two formulations, the one lacking a surfactant and the one containing Pxl88, showed clearly less tendency for SO detachment. Subsequently, higher container stability was obtained with these formulations without a significant increase of extrusion forces or even failure of the syringe. The trend was observed with verum and placebo. The extrusion force results were well in line with the residual SO amount analyzed by FTIR, and the layer thickness analyzed by interferometry and 3D-LSM. As discussed previously [44] it should be noted that layer thickness measurements based on interferometry only cover a small

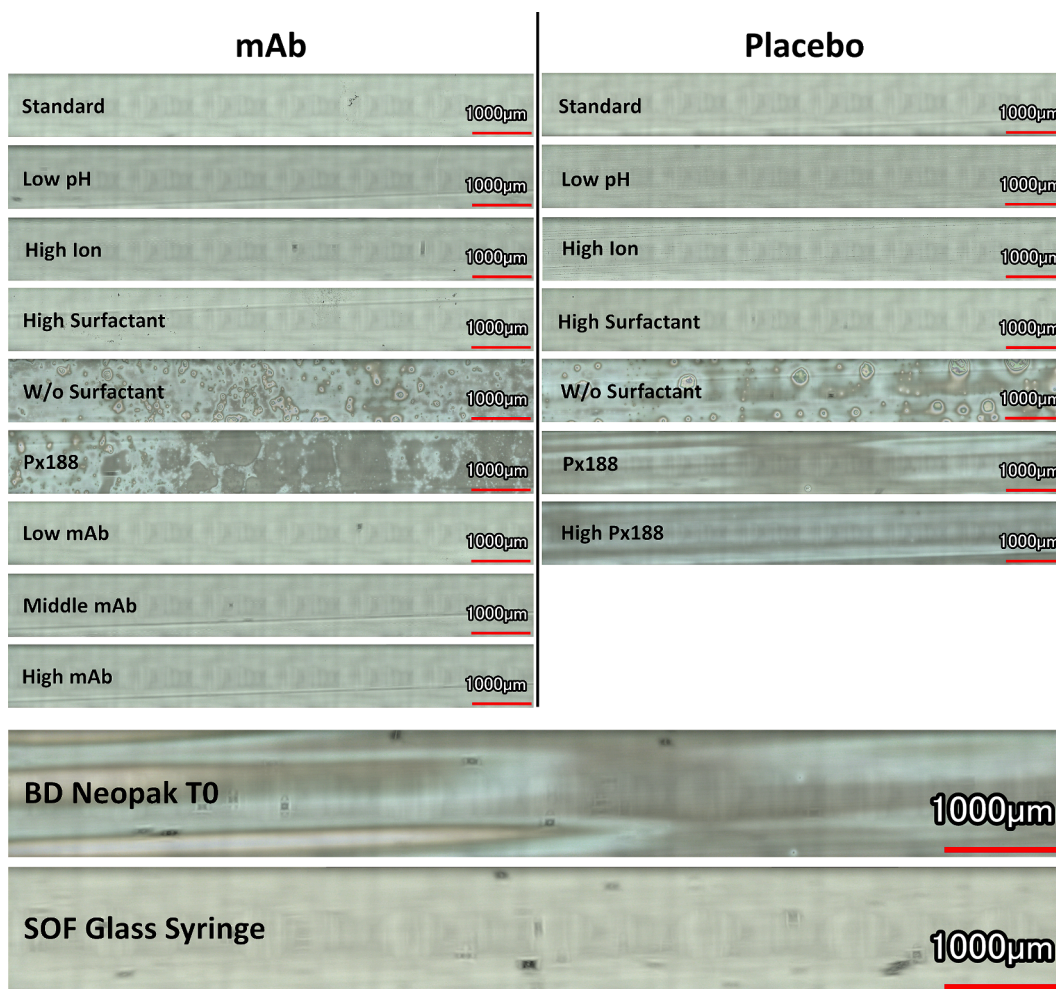


Fig. 5. 3D-LSM images of the inner surface of syringes after storage at 40 °C for 3 months of different mAb 4 and placebo formulations compared to T0 and non-silicized syringes.

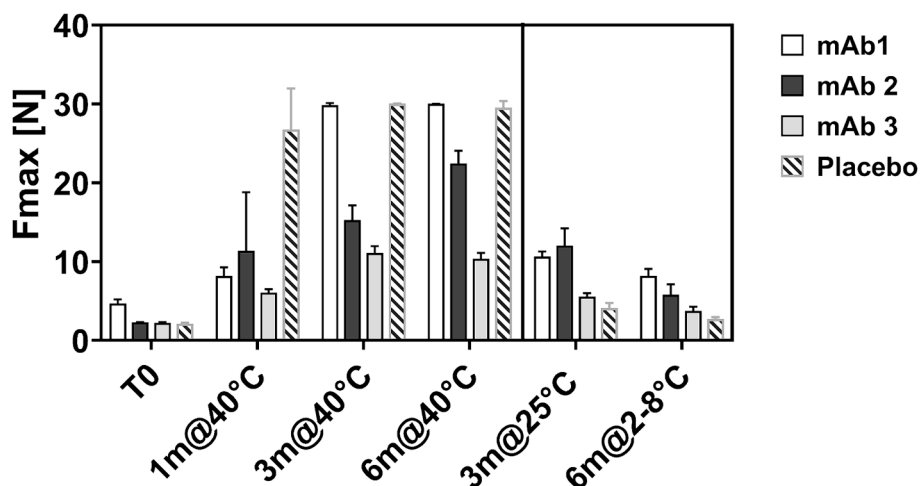


Fig. 6. Maximum extrusion forces (Fmax) of syringes after storage at 40 °C, 25 °C or 2–8 °C of mAb 1, 2 and 3 as well as placebo formulations.

section of the silicone oil surface and rely on an even silicone oil distribution. 3D-LSM turned out to be a quick, non-destructive, and reliable method to identify SO removal from the inner barrel surface. Additionally, SvP analysis showed less particles for those two formulations compared to all other formulations after expelling. Hence as reported for PS80 [16–18], also PS20 shows higher tendency to remove SO from the

container surface and to increase gliding forces in siliconized syringes compared to Px188. In comparison, a higher mAb concentration, different pH or higher ionic strength did not markedly affect the syringe stability as all PS20 containing formulations showed the same SO depletion and a distinct increase in gliding forces at the 3 months timepoint. However, for the verum the SO removal was slightly

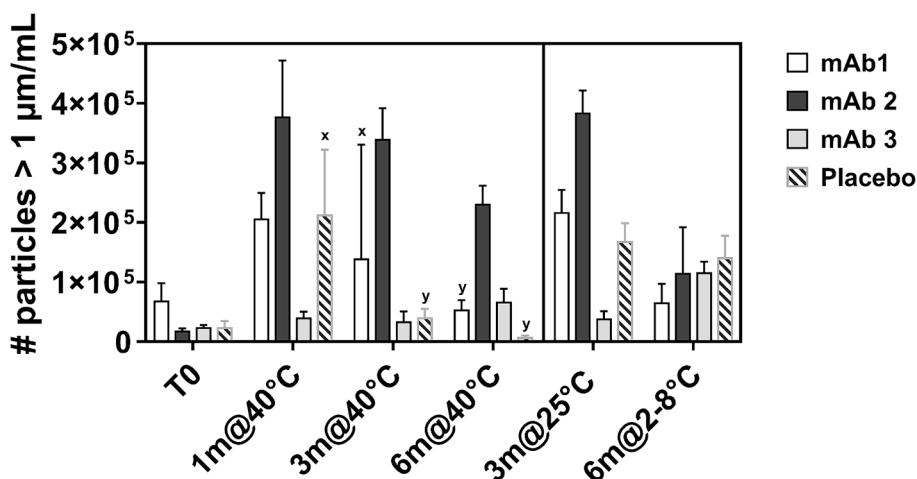


Fig. 7. Number of particles > 1 μm/mL after storage at 40 °C, 25 °C or 2–8 °C of mAb 1, 2 and 3 as well as placebo formulations. x. Samples with incomplete extrusion due to functionality failure; y: all syringes failed.

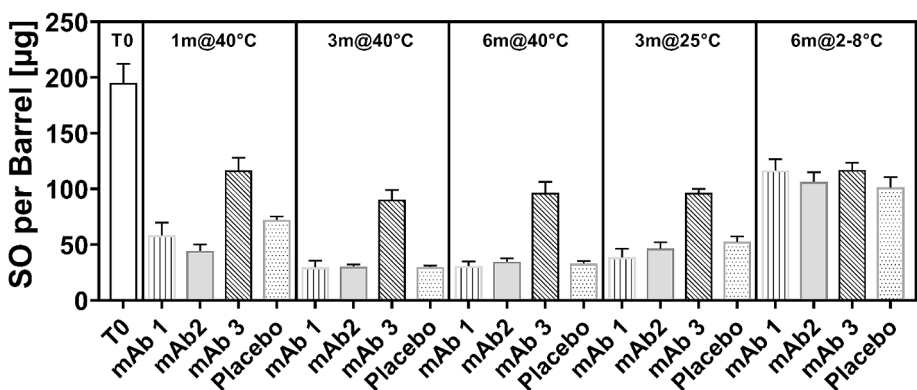


Fig. 8. SO amount per barrel by FTIR after storage at 40 °C, 25 °C or 2–8 °C of mAb 1, 2 and 3 as well as placebo formulations.

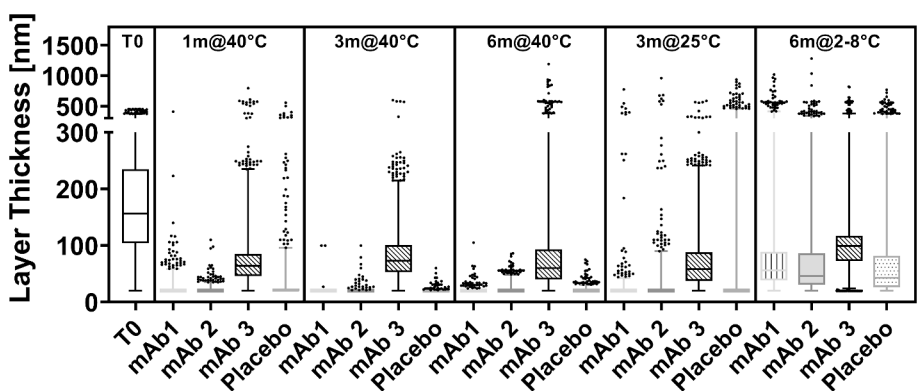


Fig. 9. SO layer thickness by WLI after storage at 40 °C, 25 °C or 2–8 °C of mAb 1, 2 and 3 as well as placebo formulations displayed as box plots (Box: 25th – 75th percentile; Whiskers: 2.5th – 97.5th percentile/LOD: 20 nm).

enhanced compared to placebo. The stability correlated with the IFT between formulation and SO, which is line with a previous report for PS 80 containing placebo formulations [17]. All PS20 containing samples displayed a lower IFT compared to the surfactant free and Px188 formulation. As the IFT decreases the energy necessary to overcome the interfacial tension is lowered and hence a SO migration is more likely to occur [17]. The formulation with highest IFT, in our case the placebo solution without surfactant, showed least silicone oil removal followed by the protein formulation without surfactant and the formulations

containing Px188. The fact that a higher PS20 concentration in the formulation did not accelerate the increase in gliding forces was also reflected in the IFT as a minimum value was already reached by the lowest PS20 concentration. The PS20 concentration of 0.06 % (w/v) is well above the critical micelle concentration (CMC) [45,46]. Px188 is less hydrophobic than PS20 with an HLB value of around 29 [30] compared to 16.7 [47], making it less surface active. Furthermore, the Px188 adsorption rate is less compared to PS20 due to its higher a molecular size around 8 kDa compared to 1.2 kDa for PS20

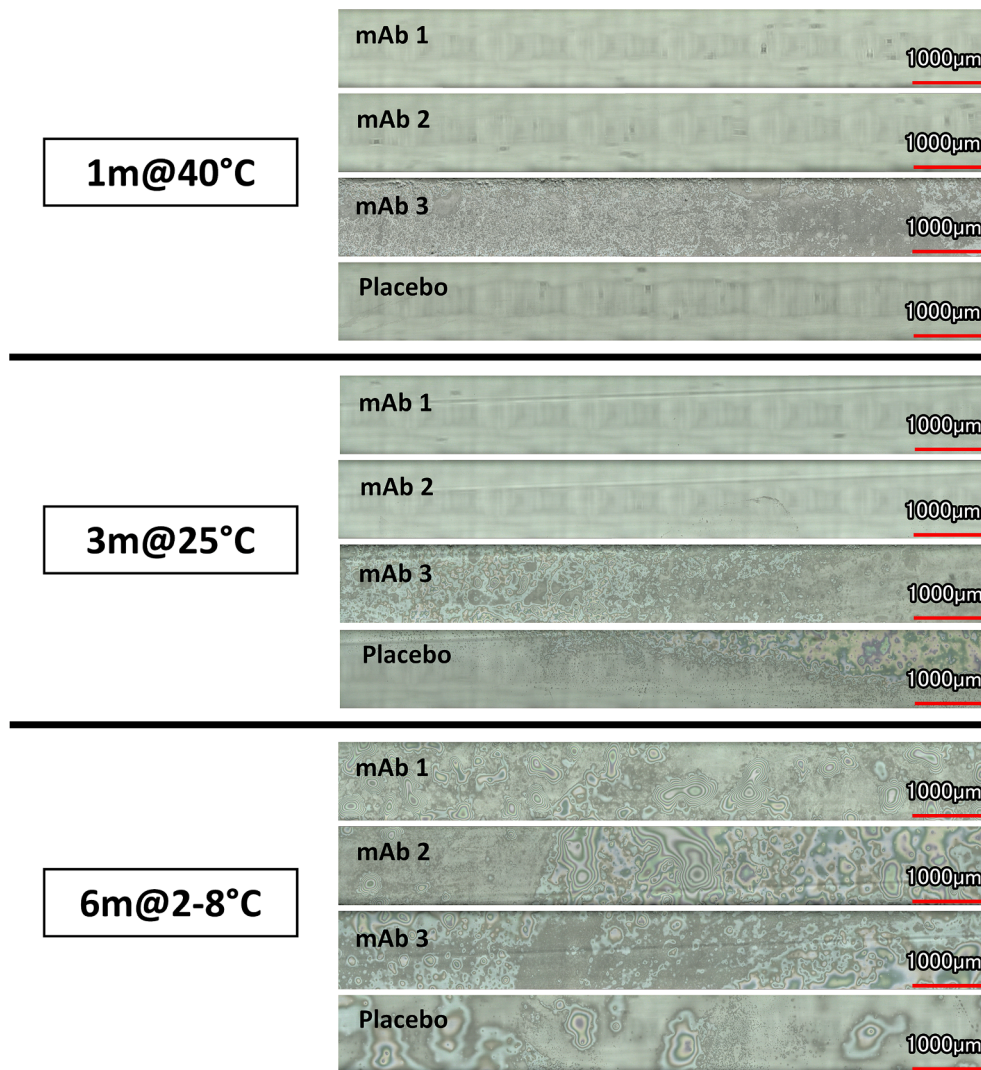


Fig. 10. 3D-LSM images of the inner surface of syringes after storage at 40 °C, 25 °C or 2–8 °C of mAb 1, 2 and 3 as well as placebo formulations.

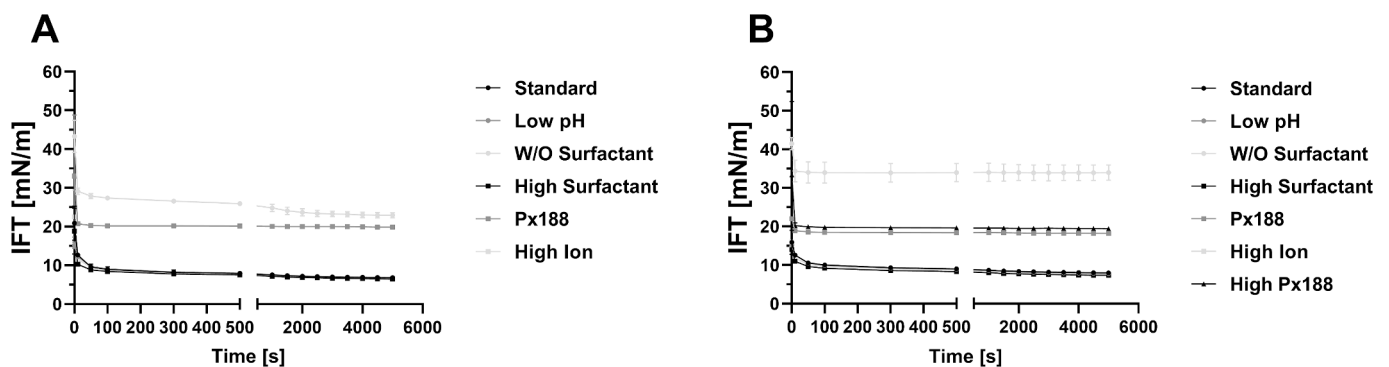


Fig. 11. IFT of different mAb 4 [A] and placebo [B] formulations at the SO interface.

[16,19,21,30,48–52]. A higher amount of protein co-adsorbed to the interface was observed for Px188 compared to polysorbates [19,25,34,51–53]. According to our results Px188 is advantageous for protein formulations in combination products. Not only did it show higher container stability but by decreasing SO migration into solution the interfacial area for mAbs to adsorb to is lower. Hence, protein stability is potentially less diminished in this case [25]. Nevertheless, the choice of surfactant needs to be evaluated based on the product itself.

Recently, visible protein-SO particles were detected after long term storage specifically in mAb formulations containing Px188.[49] After all, the occurrence of SO depletion can be also overcome by the appropriate choice of the primary packaging material [3,11,54].

In the second setup, the mAb was varied in the very same formulation (Formulation mAb 1). The stability was mAb molecule dependent. mAb 3 formulations were more stable compared to mAb 1 and 2 formulations as well as placebo at 40 °C, 25 °C and 2–8 °C. In general, SO

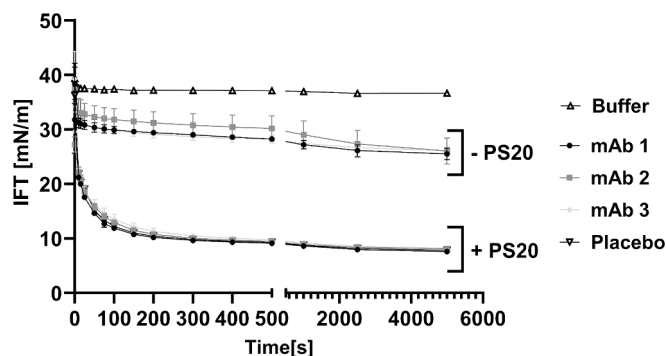


Fig. 12. IFT of formulations containing mAb 1, 2 and 3 and placebo with (+) and without (-) 0.02 % (w/v) PS20.

migration was less pronounced after storage at lower temperature. But an increase in extrusion forces and a reduction of the SO layer thickness were observed, following the 40 °C results except for placebo solutions. The sampling at 2–8 °C only covered stability up to 6 months, so further testing for 2 years and beyond would be required to verify the relevance of the observation for storage of a drug product. Considering the complete dataset, the results at accelerated storage conditions reflected the protein specific SO detachment at lower storage temperatures. Trends in differences in extrusion forces between the different formulations observed at elevated temperatures could not be simply extrapolated. Thus, it is recommended to include SO layer characterization during stability testing to properly evaluate the risk for container functionality failure upon long-term storage. In contrast to the formulation factor study as well as previous reports [16,17], the stability behaviour did not correlate to the IFT results. We assume a decreased IFT between the formulation and SO as one of the basic requirements for SO detachment. Nonetheless the protein effect on SO detachment was not reflected in IFT data. Additional dilatational surface rheology measurements did not show any differences in the behaviour of the mAb molecules at the SO interface. mAbs are known to form viscoelastic films upon adsorption at hydrophobic interfaces as a result of unfolding and increasing intermolecular interactions [22,24,25,55]. The presence of surfactant equally decreased elasticity regardless of the mAb type. A lower elasticity for protein-surfactant mixtures was expected as PS20 prevents the adsorption of the protein and thereby the formation of a protein network at the interface [27,28,51,53,56]. As the values matched the placebo, we assume the SO interface to be predominantly occupied by PS20 for all formulations. Further characterization of the protein molecules failed to identify clear predictive parameters related to SO detachment. Conformational stability, as tested via thermal unfolding, did not correlate with the stability of the syringes. Upon adsorption conformational changes of proteins can occur and an increased conformational stability tested both by thermal and chemical means is in general associated with a lower

adsorption tendency [35,38]. Only the relative hydrophobicity ranking was in line with the stability data. Hydrophobic interactions play a substantial role for protein adsorption to solid surfaces and thus an increased surface hydrophobicity could potentially enhance the interaction between the mAb and the SO interface respectively SO microdroplets in solution [34,40,57,58].

However, a different adsorption behaviour of the mAb molecules was not indicated by the dynamic IFT measurements. Thus, the mechanism behind the stabilization respectively destabilization remains unclear at this point. In general, the results illustrate the importance to include active pharmaceutical ingredients in container stability testing as well as for investigational studies on SO migration in primary containers. Recent publications on this matter often tested placebo or surrogate solutions only [15,17,18]. A broad variety of different methods can be applied to further investigate the adsorption behaviour of the protein and surfactant at the SO interface as well as the reversibility of the adsorption process [35,59,60]. Especially quartz crystal microbalance with dissipation monitoring (QCM-D) has been utilized to study the adsorption of proteins and surfactants to siliconized surfaces and it also offers to determine a viscoelasticity of the adsorbed film [19,30,40]. In general, the monitoring of adsorption and desorption kinetics of the proteins to hydrophobic surfaces by methods like ellipsometry [61], optical waveguide lightmode spectroscopy [21], surface plasmon resonance [62] or bilayer interferometry [63] could help identify key differences for the molecules. Also, neutron reflectometry has been used to study the adsorption behaviour to hydrophobic surfaces as it can provide detailed information about the molecule orientation and composition of the adsorbed film by determining layer thickness in the sub nanometer range [51,52,64,65]. The inclusion of more proteins with a broader variety of physico-chemical and surface-active properties is needed to identify the key factors influencing the SO detachment from the inner barrel surface. As all mAbs included in this study belonged to the IgG₁ subclass we expect no significant difference of the Fc fragment between the molecules [66]. A focus on the characterization of the Fab fragments could potentially facilitate the identification of predictive molecule properties. Finally, we suggest studies that focus on the interaction of the surfactants, SO and the protein beyond the interfacial properties of the formulations as the surface rheology measurements indicated the absence of the mAb molecule at the interface. Potentially, the ability to emulsify SO microdroplets plays a role in the SO migration enhancing tendency of certain formulations and mAb molecules. This could explain the lower stabilities of placebo formulations at higher storage temperature as the CMC of PS decreases and the micelle size increases at elevated temperatures [67,68]. In addition, mAbs were shown to increase the CMC of PS20 and PS80 due to interaction between protein and surfactant [69,70]. The fact that Px188 exhibits a significantly higher CMC than PS may also be in line with a higher SO layer stability due to less microdroplet formation [16,34,71].

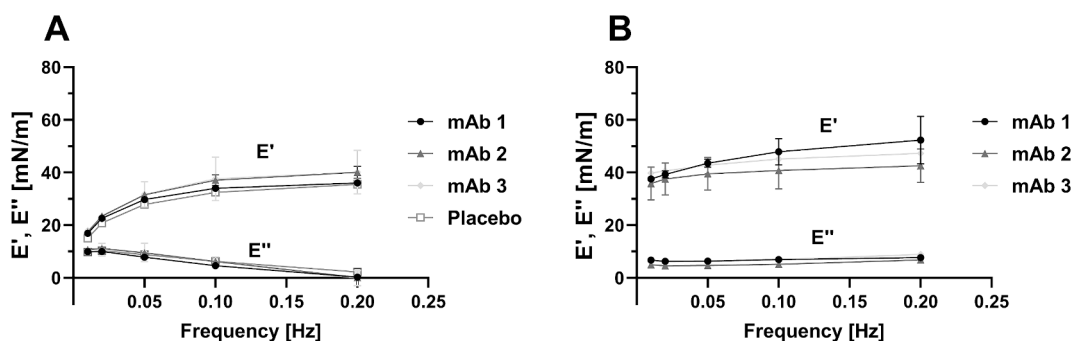


Fig. 13. Dilatational storage (E') and loss modulus (E'') of the interfacial film between SO and formulations containing mAb 1, 2 and 3 and placebo with [A] and without [B] 0.02 % (w/v) PS20 at different oscillation frequencies.

5. Conclusion

In the course of this study the dependency of the container stability on the fill medium systems became evident for standard spray-on siliconized container. In general, extrusion forces increased due to SO migration into the drug product at all storage temperatures including samples stored at 2–8 °C. Differences between formulations were already detectable after one month storage at 40 °C, which was predictive for storage at 25 °C and 2–8 °C. The silicone layer characterization revealed a complete SO removal from the inner barrel surface for specific formulations. Not only surfactant type but interestingly also the mAb present in formulation were found to impact container stability. Px188 containing formulations showed less SO detachment compared to PS20 containing formulations. mAb 3 samples were significantly more stable compared to syringes filled with mAb 1 and 2 and compared to placebo. In the case of formulation variables, a lower container stability could be correlated with a lower IFT, but the IFT did not differ with the mAb utilized. Also, interfacial rheology measurements as well as protein characterization in terms of conformational stability could not explain the difference between the mAbs in the very same formulation. Although the hydrophobicity ranking indicates that the observed SO depletion can be linked to intrinsic molecule properties, further studies are necessary to better understand the role of the protein in the SO detachment process and identify key factors for the occurrence of SO depletion. Overall, the studies underline the importance of testing container stability with verum.

CRedit authorship contribution statement

Fabian Moll: Writing – original draft, Writing – review & editing, Investigation, Formal analysis, Data curation, Conceptualization. **Karoline Bechtold-Peters:** Writing – review & editing, Supervision. **Wolfgang Friess:** Writing – review & editing, Supervision.

Declaration of competing interest

The authors declare that they have no known competing financial interests or personal relationships that could have appeared to influence the work reported in this paper.

Data availability

Data will be made available on request.

Acknowledgements

This work was funded by the Novartis AG, Basel. We also thank Omaira Missaoui for supporting with some measurements for the formulation dependent stability study as well as interfacial tension measurements.

Appendix A. Supplementary data

Supplementary data to this article can be found online at <https://doi.org/10.1016/j.ejpb.2024.114418>.

References

- N.W. Warne, H.C. Mahler, Challenges in protein product development, in: *AAPS Advances in the Pharmaceutical Sciences Series*, Vol. 38., Springer, Cham, 2018, <https://doi.org/10.1007/978-3-319-90603-4>.
- F. Jameel, J.W. Skoug, R.R. Nesbitt, Development of Biopharmaceutical Drug-Device Products, in: F. Jameel, J.W. Skoug, R.R. Nesbitt (Eds.), *AAPS Advances in the Pharmaceutical Sciences Series*, Springer International Publishing, Cham, vol. 35, 2020. Doi: 10.1007/978-3-030-31415-6.
- S. Yoneda, T. Torisu, S. Uchiyama, Development of syringes and vials for delivery of biologics: current challenges and innovative solutions, *Expert Opin. Drug Deliv.* 18 (4) (2021) 459–470, <https://doi.org/10.1080/17425247.2021.1853699>.
- G. Sacha, J.A. Rogers, R.L. Miller, Pre-filled syringes: a review of the history, manufacturing and challenges, *Pharm. Dev. Technol.* 20 (1) (2015) 1–11, <https://doi.org/10.3109/10837450.2014.982825>.
- G.A. Sacha, W. Saffell-Clemmer, K. Abram, M.J. Akers, Practical fundamentals of glass, rubber, and plastic sterile packaging systems, *Pharm. Dev. Technol.* 15 (1) (2010) 6–34, <https://doi.org/10.3109/10837450903511178>.
- A. Gerhardt, N.R. McGraw, D.K. Schwartz, J.S. Bee, J.F. Carpenter, T.W. Randolph, Protein aggregation and particle formation in prefilled glass syringes, *J. Pharm. Sci.* 103 (6) (2014) 1601–1612, <https://doi.org/10.1002/jps.23973>.
- P. Basu, A.W. Blake-Haskins, K.B. O'Berry, T.W. Randolph, J.F. Carpenter, Albinterferon A2b adsorption to silicone oil-water interfaces: effects on protein conformation, aggregation, and subvisible particle formation, *J. Pharm. Sci.* 103 (2) (2014) 427–436, <https://doi.org/10.1002/jps.23821>.
- C.F. Chisholm, A.E. Baker, K.R. Soucie, R.M. Torres, J.F. Carpenter, T.W. Randolph, Silicone oil microdroplets can induce antibody responses against recombinant murine growth hormone in mice, *J. Pharm. Sci.* 105 (5) (2016) 1623–1632, <https://doi.org/10.1016/j.xphs.2016.02.019>.
- C.F. Chisholm, K.R. Soucie, J.S. Song, P. Strauch, R.M. Torres, J.F. Carpenter, J. A. Ragheb, T.W. Randolph, Immunogenicity of structurally perturbed hen egg lysozyme adsorbed to silicone oil microdroplets in wild-type and transgenic mouse models, *J. Pharm. Sci.* 106 (6) (2017) 1519–1527, <https://doi.org/10.1016/j.xphs.2017.02.008>.
- G.B. Melo, N.F.S. da Cruz, G.G. Emerson, F.A. Rezende, C.H. Meyer, S. Uchiyama, J. Carpenter, H.F. Shiroma, M.E. Farah, M. Maia, E.B. Rodrigues, Critical analysis of techniques and materials used in devices, syringes, and needles used for intravitreal injections, *Prog. Retin. Eye Res.* 80 (March) (2021), <https://doi.org/10.1016/j.preteyeres.2020.100862>.
- S. Funke, J. Matilainen, H. Nalenz, K. Bechtold-Peters, H.-C. Mahler, F.W. Silicone, M.-O. Layers, Particle characterization in placebo and protein solutions, *J. Pharm. Sci.* 105 (12) (2016) 3520–3531, <https://doi.org/10.1016/j.xphs.2016.08.031>.
- A. Gerhardt, B.H. Nguyen, R. Lewus, J.F. Carpenter, T.W. Randolph, Effect of the siliconization method on particle generation in a monoclonal antibody formulation in pre-filled syringes, *J. Pharm. Sci.* 104 (5) (2015) 1601–1609, <https://doi.org/10.1002/jps.24387>.
- R.A. Depaz, T. Chevolleau, S. Jouffray, R. Narwal, M.N. Dimitrova, Cross-linked silicone coating: a novel prefilled syringe technology that reduces subvisible particles and maintains compatibility with biologics, *J. Pharm. Sci.* 103 (5) (2014) 1383–1393, <https://doi.org/10.1002/jps.23947>.
- A. Chillon, A. Pace, D. Zuccato, Introducing the Alba® primary packaging platform. Part 1: Particle release evaluation, *PDA J. Pharm. Sci. Technol.* 72 (4) (2018) 382–392, <https://doi.org/10.5731/pdajpst.2018.008623>.
- G.H. Shi, G. Gopalrathnam, S.L. Shinkle, X. Dong, J.D. Hofer, E.C. Jensen, N. Rajagopalan, Impact of drug formulation variables on silicone oil structure and functionality of prefilled syringe system, *PDA J. Pharm. Sci. Technol.* 72 (1) (2018) 50–61, <https://doi.org/10.5731/pdajpst.2017.008169>.
- T. Wang, C.A. Richard, X. Dong, G.H. Shi, Impact of surfactants on the functionality of prefilled syringes, *J. Pharm. Sci.* (2020) 1–10, <https://doi.org/10.1016/j.xphs.2020.07.033>.
- C.A. Richard, T. Wang, S.L. Clark, Using first principles to link silicone oil / formulation interfacial tension with syringe functionality in pre-filled syringes systems, *J. Pharm. Sci.* (2020), <https://doi.org/10.1016/j.xphs.2020.06.014>.
- L. Fang, C.A. Richard, G.H. Shi, X. Dong, M.C. Rase, T. Wang, Physicochemical excipient-container interactions in prefilled syringes and their impact on syringe functionality, *pdajpst.2020.012278*, *PDA J. Pharm. Sci. Technol.* (2021), <https://doi.org/10.5731/pdajpst.2020.012278>.
- N. Dixit, K.M. Maloney, D.S. Kalonia, Protein-silicone oil interactions: comparative effect of nonionic surfactants on the interfacial behavior of a fusion protein, *Pharm. Res.* 30 (7) (2013) 1848–1859, <https://doi.org/10.1007/s11095-013-1028-1>.
- F. Begum, S. Amin, Investigating the influence of polysorbate 20/80 and poloxamer P188 on the surface & interfacial properties of bovine serum albumin and lysozyme, *Pharm. Res.* 36 (7) (2019), <https://doi.org/10.1007/s11095-019-2631-6>.
- H.L. Kim, A. Mcauley, B. Livesay, W.D. Gray, J. Mcguire, Modulation of protein adsorption by poloxamer 188 in relation to polysorbates 80 and 20 at solid surfaces, *J. Pharm. Sci.* 103 (4) (2014) 1043–1049, <https://doi.org/10.1002/jps.23907>.
- S.B. Mehta, R. Lewus, J.S. Bee, T.W. Randolph, J.F. Carpenter, Gelation of a monoclonal antibody at the silicone oil-water interface and subsequent rupture of the interfacial gel results in aggregation and particle formation, *J. Pharm. Sci.* 104 (4) (2015) 1282–1290, <https://doi.org/10.1002/jps.24358>.
- R. Thirumangalathu, S. Krishnan, M.S. Ricci, D.N. Brems, T.W. Randolph, J. F. Carpenter, Silicone oil- and agitation-induced aggregation of a monoclonal antibody in aqueous solution, *J. Pharm. Sci.* 98 (9) (2009) 3167–3181, <https://doi.org/10.1002/jps.21719>.
- E.M. Freer, K.S. Yim, G.G. Fuller, C.J. Radke, Interfacial rheology of globular and flexible proteins at the hexadecane/water interface: comparison of shear and dilatation deformation, *J. Phys. Chem. B* 108 (12) (2004) 3835–3844, <https://doi.org/10.1021/jp037236k>.
- A. Kannan, I.C. Shieh, P.G. Negulescu, V. Chandran Suja, G.G. Fuller, Adsorption and aggregation of monoclonal antibodies at silicone oil-water interfaces, *Mol. Pharm.* 18 (4) (2021) 1656–1665, <https://doi.org/10.1021/acs.molpharmaceut.0c01113>.
- A. Kannan, I.C. Shieh, G.G. Fuller, Linking aggregation and interfacial properties in monoclonal antibody-surfactant formulations, *J. Colloid Interface Sci.* 550 (2019) 128–138, <https://doi.org/10.1016/j.jcis.2019.04.060>.

- [27] A.M. Bos, T. van Vliet, Interfacial rheological properties of adsorbed protein layers and surfactants: a review, *Adv. Colloid Interface Sci.* 91 (3) (2001) 437–471, [https://doi.org/10.1016/S0001-8686\(00\)00077-4](https://doi.org/10.1016/S0001-8686(00)00077-4).
- [28] W.J. Mcauley, D.S. Jones, V.L. Kett, Characterisation of the interaction of lactate dehydrogenase with tween-20 using isothermal titration calorimetry, interfacial rheometry and surface tension measurements, *J. Pharm. Sci.* 98 (8) (2009) 2659–2669, <https://doi.org/10.1002/jps.21640>.
- [29] N. Jiao, G.V. Barnett, T.R. Christian, L.O. Narhi, N.H. Joh, M.K. Joubert, S. Cao, Characterization of subvisible particles in biotherapeutic prefilled syringes: the role of polysorbate and protein on the formation of silicone oil and protein subvisible particles after drop shock, *J. Pharm. Sci.* 109 (1) (2020) 640–645, <https://doi.org/10.1016/j.xphs.2019.10.066>.
- [30] J. Li, S. Pinnamaneni, Y. Quan, A. Jaiswal, F.I. Andersson, X. Zhang, Mechanistic understanding of protein-silicone oil interactions, *Pharm. Res.* 29 (6) (2012) 1689–1697, <https://doi.org/10.1007/s11095-012-0696-6>.
- [31] E. Köpf, Antibody drugs at the liquid-air interface: physicochemical characteristics, aggregation & the impact of formulation. Ph.D. Thesis, LMU Munich, 2017.
- [32] N. Dixit, K.M. Maloney, D.S. Kalonia, The effect of Tween® 20 on silicone oil-fusion protein interactions, *Int. J. Pharm.* 429 (1–2) (2012) 158–167, <https://doi.org/10.1016/j.ijpharm.2012.03.005>.
- [33] A. Kannan, I.C. Shieh, D.L. Leiske, G.G. Fuller, Monoclonal antibody interfaces: dilatation mechanics and bubble coalescence, *Langmuir* 34 (2) (2018) 630–638, <https://doi.org/10.1021/acs.langmuir.7b03790>.
- [34] K. Höger, J. Mathes, W. Frieß, IgG1 adsorption to siliconized glass vials-influence of pH, ionic strength, and nonionic surfactants, *J. Pharm. Sci.* 104 (1) (2015) 34–43, <https://doi.org/10.1002/jps.24239>.
- [35] M. Rabe, D. Verdes, S. Seeger, Understanding protein adsorption phenomena at solid surfaces, *Adv. Colloid Interface Sci.* 162 (1–2) (2011) 87–106, <https://doi.org/10.1016/j.cis.2010.12.007>.
- [36] A. Gerhardt, K. Bonam, J.S. Bee, J.F. Carpenter, T.W. Randolph, Ionic strength affects tertiary structure and aggregation propensity of a monoclonal antibody adsorbed to silicone oil-water interfaces, *J. Pharm. Sci.* 102 (2013) 429–440, <https://doi.org/10.1002/jps.23408>.
- [37] D.B. Ludwig, J.F. Carpenter, J.-B. Hamel, T.W. Randolph, Protein adsorption and excipient effects on kinetic stability of silicone oil emulsions, *J. Pharm. Sci.* 99 (4) (2010) 1721–1733, <https://doi.org/10.1002/jps>.
- [38] M. Karlsson, J. Ekeröth, H. Elwing, U. Carlsson, Reduction of irreversible protein adsorption on solid surfaces by protein engineering for increased stability, *J. Biol. Chem.* 280 (27) (2005) 25558–25564, <https://doi.org/10.1074/jbc.M503665200>.
- [39] W. Norde, Driving forces for protein adsorption at solid surfaces, *Macromol. Symp.* 103 (1996) 5–18, <https://doi.org/10.1002/masy.19961030104>.
- [40] A. Oom, M. Poggi, J. Wikström, M. Sukumar, Surface interactions of monoclonal antibodies characterized by quartz crystal microbalance with dissipation: impact of hydrophobicity and protein self-interactions, *J. Pharm. Sci.* 101 (2) (2012) 519–529, <https://doi.org/10.1002/jps.22771>.
- [41] S. Funke, J. Mattilainen, H. Nalenz, K. Bechtold-Peters, H.-C. Mahler, W. Friess, Analysis of thin baked-on silicone layers by FTIR and 3D-laser scanning microscopy, *Eur. J. Pharm. Biopharm.* 96 (2015) 304–313, <https://doi.org/10.1016/j.ejpb.2015.08.009>.
- [42] H. Svilenov, U. Markoja, G. Winter, Isothermal chemical denaturation as a complementary tool to overcome limitations of thermal differential scanning fluorimetry in predicting physical stability of protein formulations, *Eur. J. Pharm. Biopharm.* 125 (January) (2018) 106–113, <https://doi.org/10.1016/j.ejpb.2018.01.004>.
- [43] M. Niklasson, C. Andresen, S. Helander, M.G.L. Roth, A. Zimdahl Kahlin, M. Lindqvist Appell, L.-G. Mårtensson, P. Lundström, Robust and convenient analysis of protein thermal and chemical stability, *Protein Sci.* 24 (12) (2015) 2055–2062, <https://doi.org/10.1002/pro.2809>.
- [44] F. Moll, K. Bechtold-Peters, W. Friess, Impact of autoclavation on baked-on siliconized containers for biologics, *Eur. J. Pharm. Biopharm.* 187 (2023) 184–195, <https://doi.org/10.1016/j.ejpb.2023.04.018>.
- [45] S. Deechongkit, J. Wen, L.O. Narhi, Y. Jiang, S.S. Park, J. Kim, B.A. Kerwin, Physical and biophysical effects of polysorbate 20 and 80 on darbepoetin alfa, *J. Pharm. Sci.* 98 (9) (2009) 3200–3217, <https://doi.org/10.1002/jps.21740>.
- [46] S. Horiuchi, G. Winter, CMC determination of nonionic surfactants in protein formulations using ultrasonic resonance technology, *Eur. J. Pharm. Biopharm.* 92 (2015) 8–14, <https://doi.org/10.1016/j.ejpb.2015.02.005>.
- [47] R. Rowe, P. Sheskey, M. Quinn, *Handbook of Pharmaceutical Excipients*, Pharmaceutical Press, London, 2009.
- [48] P. Kolliphor, M. Poloxamer, M. Poloxamer, *Technical information sheet kolliphor® P 188, BASF SE* (2021) 1–4.
- [49] C. Grapentin, C. Müller, R.S.K. Kishore, M. Adler, I. ElBialy, W. Friess, J. Huwyler, T.A. Khan, Protein-polydimethylsiloxane particles in liquid vial monoclonal antibody formulations containing poloxamer 188, *J. Pharm. Sci.* 109 (8) (2020) 2393–2404, <https://doi.org/10.1016/j.xphs.2020.03.010>.
- [50] Sigma-Aldrich Chemie GmbH. Sicherheitsdatenblatt Gemäß Verordnung (EG) Nr. 1907/2006 Tween® 20, 2021, pp. 1–9.
- [51] Y.S. Tein, Z. Zhang, N.J. Wagner, Competitive surface activity of monoclonal antibodies and nonionic surfactants at the air-water interface determined by interfacial rheology and neutron reflectometry, *Langmuir* 36 (27) (2020) 7814–7823, <https://doi.org/10.1021/acs.langmuir.0c00797>.
- [52] Z. Zhang, A. Marie Woys, K. Hong, C. Grapentin, T.A. Khan, I.E. Zarraga, N. J. Wagner, Y. Liu, Adsorption of non-ionic surfactant and monoclonal antibody on siliconized surface studied by neutron reflectometry, *J. Colloid Interface Sci.* 584 (2020) 429–438, <https://doi.org/10.1016/j.jcis.2020.09.110>.
- [53] A.R. Narváez, S.V. Vaidya, Protein-surfactant interactions at the air-water interface, in: *Excipient Applications in Formulation Design and Drug Delivery*, Springer International Publishing, Cham, 2015, pp. 139–166, https://doi.org/10.1007/978-3-319-20206-8_6.
- [54] K. Yoshino, K. Nakamura, A. Yamashita, Y. Abe, K. Iwasaki, Y. Kanazawa, K. Funatsu, T. Yoshimoto, S. Suzuki, Functional evaluation and characterization of a newly developed silicone oil-free prefilled syringe system, *J. Pharm. Sci.* 103 (5) (2014) 1520–1528, <https://doi.org/10.1002/jps.23945>.
- [55] D.J. Burgess, N.O. Sahin, Interfacial rheological and tension properties of protein films, *J. Colloid Interface Sci.* 189 (1) (1997) 74–82, <https://doi.org/10.1006/jcis.1997.4803>.
- [56] B.R. Blomqvist, M.J. Ridout, A.R. Mackie, T. Wårnheim, P.M. Claesson, P. Wilde, Disruption of viscoelastic β -lactoglobulin surface layers at the air-water interface by nonionic polymeric surfactants, *Langmuir* 20 (23) (2004) 10150–10158, <https://doi.org/10.1021/la0485475>.
- [57] A.W.P. Vermeer, C.E. Giacomelli, W. Norde, Adsorption of IgG onto hydrophobic teflon. Differences between the Fab and Fc domains, *Biochim. Biophys. Acta - Gen. Subj.* 1526 (1) (2001) 61–69, [https://doi.org/10.1016/S0304-4165\(01\)00101-5](https://doi.org/10.1016/S0304-4165(01)00101-5).
- [58] A.D. Kanthe, M. Krause, S. Zheng, A. Ilott, J. Li, W. Bu, M.K. Bera, B. Lin, C. Maldarelli, R.S. Tu, Armoring the interface with surfactants to prevent the adsorption of monoclonal antibodies, *ACS Appl. Mater. Interfaces* 12 (8) (2020) 9977–9988, <https://doi.org/10.1021/acsami.9b21979>.
- [59] J. Li, M.E. Krause, X. Chen, Y. Cheng, W. Dai, J.J. Hill, M. Huang, S. Jordan, D. LaCasse, L. Narhi, E. Shalae, I.C. Shieh, J.C. Thomas, R. Tu, S. Zheng, L. Zhu, Interfacial stress in the development of biologics: fundamental understanding, current practice, and future perspective, *AAPS J.* 21 (3) (2019), <https://doi.org/10.1208/s12248-019-0312-3>.
- [60] K. Nakanishi, T. Sakiyama, K. Imamura, On the adsorption of proteins on solid surfaces, a common but very complicated phenomenon, *J. Biosci. Biotech.* 91 (3) (2001) 233–244, [https://doi.org/10.1016/S1389-1723\(01\)80127-4](https://doi.org/10.1016/S1389-1723(01)80127-4).
- [61] M. Malmsten, Ellipsometry studies of the effects of surface hydrophobicity on protein adsorption, *Colloids Surfaces B Biointerfaces* 3 (5) (1995) 297–308, [https://doi.org/10.1016/0927-7765\(94\)01139-V](https://doi.org/10.1016/0927-7765(94)01139-V).
- [62] L. Nault, P. Guo, B. Jain, Y. Bréchet, F. Bruckert, M. Weidenhaupt, Human insulin adsorption kinetics, conformational changes and amyloid aggregate formation on hydrophobic surfaces, *Acta Biomater.* 9 (2) (2013) 5070–5079, <https://doi.org/10.1016/j.actbio.2012.09.025>.
- [63] M.H. Ramadan, J.E. Prata, O. Karácsony, G. Dunér, N.R. Washburn, Reducing protein adsorption with polymer-grafted hyaluronic acid coatings, *Langmuir* 30 (25) (2014) 7485–7495, <https://doi.org/10.1021/la500918p>.
- [64] S. Ruane, Z. Li, M. Campana, X. Hu, H. Gong, J.R.P. Webster, F. Uddin, C. Kalonia, S.M. Bishop, C.F. Van Der Walle, J.R. Lu, Interfacial adsorption of a monoclonal antibody and its Fab and Fc fragments at the oil/water interface, *Langmuir* 35 (42) (2019) 13543–13552, <https://doi.org/10.1021/acs.langmuir.9b02317>.
- [65] R.G. Couston, M.W. Skoda, S. Uddin, C.F. Van Der Walle, Adsorption behavior of a human monoclonal antibody at hydrophilic and hydrophobic surfaces, *MAbs* 5 (1) (2013) 126–139, <https://doi.org/10.4161/mabs.22522>.
- [66] N. Chennamsetty, B. Helk, V. Voynov, V. Kayser, B.L. Trout, Aggregation-prone motifs in human immunoglobulin G, *J. Mol. Biol.* 391 (2) (2009) 404–413, <https://doi.org/10.1016/j.jmb.2009.06.028>.
- [67] J. Nayem, Z. Zhang, A. Tomlinson, I.E. Zarraga, N.J. Wagner, Y. Liu, Micellar morphology of polysorbate 20 and 80 and their ester fractions in solution via small-angle neutron scattering, *J. Pharm. Sci.* 109 (4) (2020) 1498–1508, <https://doi.org/10.1016/j.xphs.2019.12.016>.
- [68] P. Garidel, M. Blech, J. Buske, A. Blume, Surface tension and self-association properties of aqueous polysorbate 20 HP and 80 HP solutions: insights into protein stabilisation mechanisms, *J. Pharm. Innov.* 16 (4) (2021) 726–734, <https://doi.org/10.1007/s12247-020-09488-4>.
- [69] H.-C. Mahler, F. Senner, K. Maeder, R. Mueller, Surface activity of a monoclonal antibody, *J. Pharm. Sci.* 98 (12) (2009) 4525–4533, <https://doi.org/10.1002/jps.21776>.
- [70] N. Dixit, D.L. Zeng, D.S. Kalonia, Application of maximum bubble pressure surface tensiometer to study protein-surfactant interactions, *Int. J. Pharm.* 439 (1–2) (2012) 317–323, <https://doi.org/10.1016/j.ijpharm.2012.09.013>.
- [71] L.S.C. Wan, P.F.S. Lee, CMC of polysorbates, *J. Pharm. Sci.* 63 (1) (1974) 136–137, <https://doi.org/10.1002/jps.2600630136>.